

4. O. A. Schaeffer, *Report BNL-581* (Brookhaven National Laboratory, 1959).
5. A. Kaufman and W. S. Broecker, in preparation.
6. D. L. Thurber, W. S. Broecker, H. A. Potratz, R. L. Blanchard, *Science* **149**, 55 (1965).
7. D. L. Thurber, *Proc. IAEA Symp. Radioactive Dating Athens, November 1962*.
8. W. H. Sackett and H. A. Potratz, in Schlanger *et al.*, *USGS Prof. Paper 260-BB* (1963).
9. K. O. Emery, T. I. Tracey, H. S. Ladd, *USGS Prof. Paper 260-A* (1954).
10. E. Burksen, N. Kapustin, I. Potupvo, *J. Ukr. Acad. Sci.* **2**, 47 (1934).
11. F. P. Fanale and J. L. Kulp, *Amer. Mineralogist* **46**, 155 (1961).
12. D. L. Thurber, personal communication.
13. C. Grégoire, *J. Biophys. Biochem. Cytol.* **3**, 797 (1957).
14. Determined by Broecker, Kaufman, and Thurber at Lamont Geological Observatory.
15. We thank W. S. Broecker, D. L. Thurber, and A. Kaufman for helpful discussions during the preparation of this paper and for supplying many of the samples. We also acknowledge the advice and cooperation of H. S. Ladd and J. I. Tracy, Jr., USGS, who supplied most of the coral samples. R. L. Batten, American Museum of Natural History, supplied some of the pre-Pleistocene mollusk shells. We also thank P. H. Abelson and P. E. Hare, Carnegie Institution, and J. Owen, USGS, who helped us collect Miocene shells from Chesapeake Bay. Work sponsored by the AEC.

19 April 1965

Carbon Abundances in Chondritic Meteorites

Abstract. Combustion analyses of total carbon in chondritic meteorites indicate a fractionation of this element between the various types of chondrites. The median values for the percentage of carbon by weight are 0.40 for enstatite chondrites, 0.09 for olivine-bronzite chondrites, and 0.08 for olivine-hypersthene chondrites. Olivine-pigeonite chondrites show great variations in their carbon contents.

The abundances of carbon have been determined in 18 chondritic meteorites by a combustion technique. Powdered samples ranging from 0.25 to 1 g in weight were burned in an oxygen atmosphere in a LECO induction furnace. One gram of iron chips and 1 g of copper chips were added to accelerate the reaction. The combustion products were carried in the oxygen stream through a MnO₂ trap to remove any SO₂ formed, and through a catalyst furnace to convert any carbon monoxide to carbon dioxide. The total CO₂ produced was determined by a modified Orsat technique (see 1) in a LECO model 572-100 carbon analyzer, by dissolving the CO₂ from the oxygen carrier in a caustic solution and measuring the volume of CO₂ lost.

The technique gives reproducible and

accurate results, as indicated by the results on two Thorn Smith steel standards. Four analyses of one standard ranged from 0.41 to 0.43 percent carbon by weight, as compared with the standard value of 0.40, and four analyses of the second standard ranged from 0.50 to 0.51, as compared with the standard value of 0.49.

The data obtained from the abundances of carbon in enstatite, olivine-bronzite, olivine-hypersthene, and carbonaceous and noncarbonaceous olivine-pigeonite chondrites are given in Table 1. Replicate analyses on the same batch of powdered meteorite for selected samples provide an index of the reproducibility of the method.

Previous determinations of carbon in chondrites have been largely limited to the three classes of carbonaceous chondrites and the enstatite chondrites. The presence of carbon in most of these meteorites is readily apparent and hence conducive to analysis. Carbonaceous chondrites of the rarer types were not analyzed in this investigation because of their rarity and the apparently reasonable values obtained in previous analyses. Values obtained by other investigators (2-5) for the same meteorites analyzed in this investigation are indicated in Table 1.

As indicated by Table 1 and Fig. 1, in which carbon abundances reported here and abundances for carbonaceous chondrites reported by Boato (3) and Wiik (4, 5) are plotted, individual meteorites within a given classification generally show a broad range of values. This type of distribution makes a calculated mean for a meteorite group of questionable value for comparison purposes; each individual meteorite should be considered separately, and representative specimens for each class should be used in comparisons. For the specimens used in this investigation, the median values for the carbon content were: enstatite chondrites, 0.40; olivine-bronzite chondrites, 0.09; olivine-hypersthene chondrites, 0.08. These values are close to those selected by Craig (6) for the average carbon content of the olivine-bronzite (high-iron group) chondrites of 0.07 and the olivine-hypersthene (low-iron group) chondrites of 0.03 and the average value of 0.29 percent carbon selected by Wood (7) for the enstatite chondrites. It is interesting to note the parallelism of the carbon abundances in the chondritic meteorites

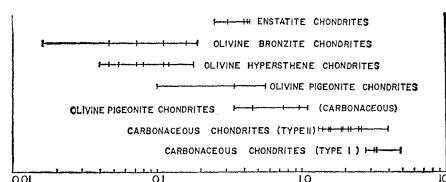


Fig. 1. Carbon distribution in chondrites (percentage by weight).

Table 1. Abundances of carbon in meteorites.

Meteorite	Abundance (% by wt.)	Previous results (% by wt.)
<i>Enstatite chondrites</i>		
Hvittis	0.25	
Khairpur	.31	0.41 (5)
Abee	.40	.38 (2)
Indarch	.41	.4 (3)
		.31 (4)
		.43 (4)
Atlanta	.43	.50 (5)
<i>Olivine-bronzite chondrites</i>		
Allegan	.014	
	.018	
Richardton	.040	0.02 (3)
	.040	
	.046	
	.049	
	.052	
Forest City	.072	0.08 (3)
	.072	
Saline	.11	
	.12	
Kesen	.15	
	.15	
	.16	
	.16	
Beardsley	.19	
<i>Olivine-hypersthene chondrites</i>		
Bruderheim	.040	
New Concord	.040	
	.046	
Leedey	.054	
Dhurmsala	.072	
	.085	
Marion, Iowa	.080	
	.085	
Farmington	.11	
	.11	
Ergheo	.11	
	.12	
Modoc	.18	
	.18	
<i>Olivine-pigeonite chondrites</i>		
Karoonda	.10	
Chainpur	.57	
Mokoia (carbonaceous)	.75	0.84 (3)
		.65 (3)
		.47 (4)

with the abundances of Hg, Tl, Pb, and Bi as noted by Reed *et al.* (8). These volatile elements are relatively depleted in the ordinary olivine-bronzite and olivine-hypersthene chondrites as compared to the enstatite, olivine-pigeonite, and carbonaceous chondrites.

CARLETON B. MOORE

CHARLES LEWIS

Arizona State University, Tempe

References and Notes

1. W. W. Scott, *Standard Methods of Chemical Analysis* (Van Nostrand, Princeton, N.J., 1939), pp. 240–241.
2. K. R. Dawson, J. A. Maxwell, D. E. Parsons, *Geochim. Cosmochim. Acta* **21**, 127 (1960).
3. G. Boato, *ibid.* **6**, 209 (1954).
4. H. B. Wiik, *ibid.* **9**, 279 (1956).
5. ———, personal communication.
6. H. Craig, in *Isotopic and Cosmic Chemistry*, H. Craig, S. L. Miller, G. J. Wasserburg, Eds. (North-Holland, Amsterdam, 1963).
7. J. Wood, in *The Moon, Meteorites and Comets*, B. M. Middlehurst and G. P. Kuiper, Eds. (Univ. of Chicago Press, Chicago, 1963).
8. G. W. Reed, K. Kogoshi, A. Turkevich, *Geochim. Cosmochim. Acta* **20**, 122 (1960).
9. Research supported in part by NASA grant NsG-399.

16 April 1965

Crystallization of Clay-Adsorbed Water

Abstract. *The nature of crystalline water in frozen pastes made from representative clay minerals and water was studied by x-ray diffraction. Only the diffraction peaks corresponding to the normal hexagonal ice structure were detected. The relative intensities of the diffraction peaks revealed evidence of epitaxy in that the ice crystals appeared to be preferentially oriented with their c-axes perpendicular to the c-axes of the individual clay crystallites.*

The tendency of an advancing ice-water interface to exclude colloidal and silt-size soil particles has been demonstrated (1). Migration of particles and other foreign bodies ahead of an advancing freezing front was partially explained by postulating the existence of a submicroscopic layer of unfrozen liquid separating the particles from the ice. The existence of this unfrozen layer of water is also vital to current theories of ice segregation and frost heaving in frozen ground. Frozen soils and clays do in fact contain significant quantities of "unfrozen water" in equilibrium with an ice phase, and the mobility of this unfrozen water in response to thermal and electrical gradients is remarkable (2), but the nature and distribution of the two phases is still imperfectly understood. In a recent discussion of the latent heat of freezing of soil water, the thermodynamic argument employed required the assumption that soil water crystallizes as normal hexagonal ice (3); this assumption accords with field and laboratory observations of segregated ground ice and appears to have been verified by x-ray methods (4), but it is questionable in view of Brzhan's report of ice of unusual structure in frozen silica gel (5).

Crystallographic data are known for four of the nine generally recognized forms of ice: the normal, hexagonal, tridymite structure; a cubic structure stable apparently only below -80°C ; and high-pressure cubic and tetragonal structures (6, 7). The first two are by far the best known. A completely amorphous form of ice that may appear when water vapor at a pressure of about 10^{-5} torr condenses on a substrate at or below -100°C and a vitreous form stable at higher temperatures also seem to be generally acknowledged. Therefore a form of ice in frozen soil or clay different from the normal tridymite structure would not be altogether surprising. As Brill (7) and others have pointed out, the geometry of the water molecule and its remarkable capacity for bonding make many configurations possible. Inasmuch as details of the study referred to by Martynov (4) have not become available and in view of the somewhat contradictory report of Brzhan (5), we have investigated the matter further.

X-ray diffraction patterns of frozen pastes of montmorillonite, kaolinite, and halloysite, in which the *c*-axes of the individual clay platelets were predominantly vertically oriented, were obtained with a Norelco x-ray diffractometer using copper $K\alpha$ radiation. During analysis the samples occupied a receptacle milled into an aluminum plate and were covered by a Mylar canopy to prevent changes in water content. Temperature of a sample was regulated by a thermoelectric module, in intimate thermal contact with the aluminum plate, in conjunction with a proportional-temperature controller actuated by a thermistor; sample temperatures were thus established at any desired values, $\pm 0.05^{\circ}\text{C}$, between 0° and -40°C . Ambient room temperature was 5°C ; this ensured no condensation of moisture on the inner surface of the Mylar canopy.

The samples were cooled rapidly to a selected temperature. Spontaneous nucleation occurred at about -5°C and the freezing front proceeded rapidly from the bottom upward and from the sides inward. Results obtained at -10°C are shown in Table 1, which also lists the data of Brzhan and the generally accepted *d*-spacings and diffraction intensities of powdered ice. The intensity data may be questioned; the difficulties in obtaining truly random crystal orientation have recently become known. However, we know of no more recent data; pending the deter-

mination of more reliable values, let us accept the ASTM data.

In every instance the *d*-spacings due to water in the frozen clays corresponded to those of normal ice, ± 0.02 Å; moreover, no anomalous, unidentifiable peaks were detected. The results in Table 1 were obtained with clays of low water content. If we assume the specific surface of montmorillonite to be $800\text{ m}^2/\text{g}$ of clay, the calculated thickness of the water films distributed over the total surface of the clay is of the order of 5 to 10 Å. When it froze, this adsorbed water evidently collected at nucleation sites where, in spite of adsorption forces, it crystallized in the normal hexagonal configuration. Numerous determinations at higher water contents and lower temperatures gave similar results; *d*-spacings detected were always attributable to hexagonal ice.

The observed relative intensities of the diffraction peaks showed consistent deviations from the random powder pattern; this fact is best explained by postulating a preferred orientation of the microscopic ice crystals in the frozen clay. During preparation of the sample, we tried to obtain preferential orientation of the individual clay platelets by repeatedly remolding the sample with a spatula. Subsequent observation of greatly enhanced (001) diffraction peaks of the montmorillonite and kaolinite clays proved that the *c*-axes of the clay platelets were preferentially oriented in the direction perpendicular to the plane of the goniometer stage.

The data of Table 1 indicate that a significant majority of the ice crystals were so oriented that their *c*-axes were in the plane parallel to that of the goniometer stage. The fact that the relative intensities of the (101), (102), (103), (112), and (203) spacings did not diminish consistently, together with the fact that relative to the (002) the (101) reflection intensified in most instances, suggests that there may be some tendency toward parallel orientation of this face; however, the main effect is still the relative intensification of the (100) reflection. On this basis one may postulate that the orientation of the clay particles was significantly effective in determining the orientation of the ice crystals in the frozen clays.

Hendricks and Jefferson, Macey, and Mathieson and Walker (8) have suggested various ways in which the configuration of the hexagonal network of oxygen atoms at the surface of silicate-clay minerals could provide both the foundation and a template on which